

EXPERIMENTAL DETERMINATION OF THE RESONANCE CONTOUR OF A THREE-LAYER INTERFEROMETER

M. A. Khashchan (Egypt)

Vestnik Moskovskogo Universiteta.
Vol. 33, No. 6, pp. 16-22, 1978

UDC 535.41:535.854

The change in the modulation depth of the interferogram of a three-layer interferometer as a function of the relative displacement of the transmission maxima of the component layers is analyzed experimentally. The fringes are displaced by rotating the interferometer with slightly wedge-shaped layers. The interferogram was recorded photoelectrically by scanning the fringes of equal inclination. The experimental relationship between the contrast of the modulation fringes and the relative displacement leads to the establishment of an analytical equation for the apparatus function of the interferometer.

Introduction. In [1] some properties of a three-layer interferometer were considered in connection with its use as a resonator, a spectrometer, a refractometer, and a comparator. In this case the interferogram of the fringes of equal chromatic order when working with a continuous spectrum determines the resonance frequencies of the interferometer. The interferogram of fringes of equal inclination when the interferometer is illuminated with monochromatic light determines the apparatus function (the resonance contour) of the interferometer. The experimental determination of this function is of considerable importance when calculating the parameters of a resonator, spectrometer, filter, etc., the actions of which are based on the use of a three-layer or multilayer interferometer.

In this paper we first record experimentally the resonance contour of a three-layer interferometer for different conditions of adjustment of two of its layers. Rotation of the three-layer interferometer, having slightly wedge-shaped thick layers, leads to scanning of the interferogram in monochromatic light when the relative displacement of the transmission fringes of the component layers is changed. Interferograms with variable modulation depth are obtained. The dependence of the modulation depth on the relative displacement of the interference fringes leads to the derivation of an equation for the resonance contour of the interferometer.

The three-layer interferometer. The three-layer interferometer consists of four plane-parallel mirrors M_1 , M_2 , M_3 and M_4 (Fig. 1), which are separated from one another by media with different refractive indices. This interferometer, for example, can be constructed using an ordinary Fabry-Perot interferometer with the plane-parallel backings of the mirrors. In our case a spacing ring of length 70 mm fixes the thickness of the air layer. The backings of the mirrors each have a geometrical thickness of 17.75 mm. They represent the first and third layers of the interferometer. One surface of each backing has a reflection coefficient of the order of 0.95. The other surface of the backing is not coated and has a low reflection coefficient of approximately 0.04, due to Fresnel reflection from the boundary of separation of the air and glass.

In a simpler form of the interferometer (Fig. 1a) the coatings of the surface of the backings are turned toward one another so that the middle air layer has high selectivity. The front and back glass layers of the interferometer have low selectivity. In this case the transmission fringes of the middle layer are many times narrower than the fringes of the outer layers, and the interferogram consists of three forms of fringes. Each form of the fringes belongs only to one layer. In Fig. 1b the uncoated surface of one backing is turned toward the coated surface of the other backing. In this case in addition to the transmission fringes of each individual layer interference fringes corresponding to the path differences equal to the sum of the path differences in the two adjacent layers with low selectivities are also obtained. In Fig. 1c the uncoated surfaces of the backings are

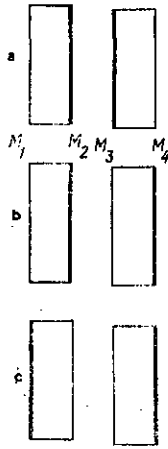


Fig. 1. Versions of the three-layer interferometer. The rectangles represent the plates, while the thick lines represent the coated surfaces.

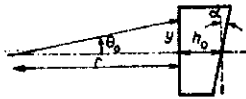


Fig. 2. Determination of the relation between the angle of rotation and the path difference in a wedge-shaped plate.

turned toward one another while the coated surfaces become end mirrors. In this case the most complex interferogram is obtained, from which one can recognize the transmission fringes of each individual layer together with fringes for the path differences equal to the sum of the path differences in the two or three adjacent layers. For the accurate identification of the different fringes the relations of the free dispersion regions for the known thicknesses are used [2]. Henceforth, the experimental results will be analyzed only in the case of an interferometer with a middle layer of high selectivity (Fig. 1a).

The three-layer interferometer considered here enables the shift of the transmission fringes of its layers with respect to one another to be monitored. The glass plates of the interferometer are slightly wedge shaped, which enables the transmission fringes of these plates to be displaced by rotating the interferometer in a plane coinciding with the principal cross sections of the wedges. As a result of this one can record the resonance contour of the interferometer both in the case of coincidence (adjustment), and in the case of noncoincidence (maladjustment) of the transmission fringes of the component layers.

The relative displacement of the transmission contours can be calculated in terms of quantities measured from the interferogram. For this purpose it is very important that the wedge-shaped plate should have a variable optical thickness l (Fig. 2) which obeys the linear relation $l = n(h_0 + \alpha y)$, where h_0 is the geometrical thickness along an axis perpendicular to y , α is the angle of the wedge, and n is the refractive index of the plate. The relation between the ordinate y and the radius of rotation r is given by the equation $y = r \operatorname{tg} \theta_0$, where θ_0 is the angle of observation. Hence, the path difference in the case of fringes of equal inclination $2l \cos \theta = 2n(h_0 \pm \alpha r |\operatorname{tg} \theta_0|) \cos \theta$, where θ is the angle of refraction inside the plate.

Consequently, the path difference inside the wedge-shaped layers does not have the same values for absolute values of the angle of observation. This means that the wedge-shaped form of the plate leads to a displacement of its fringes relative to the fringes observed in the case when it is plane-parallel. The relative displacement of the fringes of the external layers can be expressed in terms of the fraction of order δp

$$\delta p = \frac{2n^2}{\lambda} (\alpha_3 r_3 - \alpha_1 r_1) \sqrt{\frac{2q}{p_0} - \left(\frac{2q}{p_0}\right)^2} \quad (1)$$

where λ is the wavelength, p_0 is the axial interference order of the middle layer, and q is the number of the angular fringe of the middle layer on the interferogram, measured from the center (q is assumed to be zero). Equation (1) will be used below with the following substitutions: the radii of rotation of the first and third layers $r_1 = 2$ cm and $r_3 = 10.77$ cm, and the angles of the wedges $\alpha_1 = \lambda/10$ and $\alpha_3 = \lambda/4.5$, where $\lambda = 6328$ Å.

The interferogram. The fringes of equal inclination with the wedge-shaped layers become accessible to observation if half the angle of the first diffraction minimum at the exit aperture is greater than the angle of the wedge [3]. In this work the incident parallel beam had a cross section of diameter 50 mm, and when the entrance and exit apertures are in the form of square openings they had sides of 10 mm. The beam cross section assigned by the helium-neon laser was increased using a reversed telescopic system. The multimode radiation was generated in a confocal resonator of length 116.5 cm. The modes covered a spectral range of width 0.01 Å. The frequencies of the modes were subject to random fluctuations which led to a reduction in the degree of monochromaticity. In this case the laser beam was considered in the form of a spectral line of width equal to the

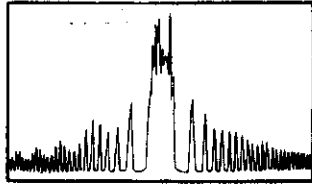


Fig. 3. Interferogram in the case when the principal section of the wedge coincides with the plane of rotation of the interferometer. Some modes of the laser are resolved in the center.

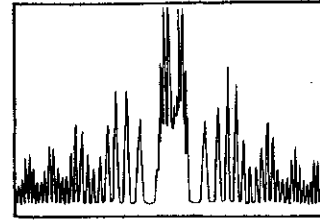


Fig. 4. Interferogram in the case when the edge of the wedge coincides with the plane of rotation of the interferometer. The modes of the laser are only resolved in the central order.

spectral range of all the generated modes.

Fringes of equal inclination were recorded photoelectrically when the interferometer was rotated in a plane perpendicular to the slit of the spectrometer, with which the interferometer was crossed. An ISP-51 prism spectrometer was used as the preliminary-dispersion spectrometer. The slit of the spectrometer had a width of $5 \mu\text{m}$ and a height of 0.5 mm . The plane of the slit coincided with the plane of localization of the fringes of equal inclination, i.e., with the focal plane of the objective of focal length 30 cm . Hence, the intensity of the light passing through the interferometer as a function of the angle of inclination was converted into a function of time. The latter in turn was converted into a function of the coordinates of the tape of the FEP-1 attachment. Recordings of the latter function are shown in Figs. 3 and 4.

The interferogram shown in Fig. 3 was recorded when the principal section of the wedge coincided with the plane of rotation. When the interferogram shown in Fig. 4 was recorded the principal plane of the wedge was perpendicular to the plane of rotation. Both interferograms consist of narrow fringes which are subjected to modulation in the form of broad fringes. The narrow fringes belong to the middle air layer of high selectivity, while the wide fringes belong to the glass layers with low selectivity. The interferogram shown in Fig. 3 has the feature that the modulation depth varies from one side of the interferogram to the other. On this interferogram it can be seen that the wide bands are suppressed on one side and increased on the other side. The modulation depth of the interferogram of Fig. 4 is the same everywhere. The advantage of an interferogram with variable modulation depth is the fact that the suppressed and amplified fringes are compared in one and the same intensity scale.

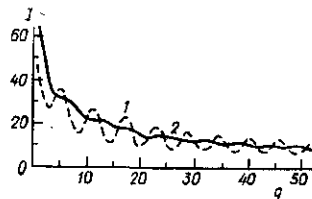


Fig. 5. Experimental relation between the intensity I of the angular maxima of the middle layer and their numbers.

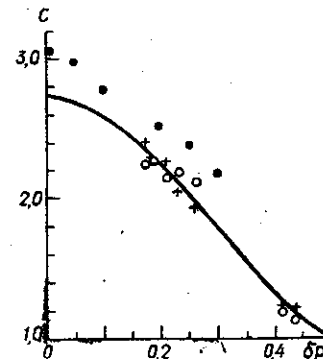


Fig. 6. Experimental (the points) and theoretical (the continuous curve) relations between the modulation depth and the relative displacement of the fringes of the first and third layers.

The contours of the nonsuppressed and suppressed broad fringes are shown in Fig. 5 (curves 1 and 2 respectively). These curves show the relation between the maximum intensity (on an arbitrary intensity scale I) of the angular orders of the middle air layer and the numbers q of these fringes. It follows from Fig. 5 that the curve of the suppressed fringes lies halfway between the maxima and minima of the unsuppressed fringes on the in-

tensity scale. The curves in Fig. 5 enable one to construct the experimental relation between the contrast C of the fringes due to interaction with the glass layers, and the relative displacement δp . This relation is compared with the theoretical calculations in order to derive accurately an expression for the resonance contour of a multilayer interferometer.

The crosses and circles in Fig. 6 indicate the values of the contrast, measured using two interferograms with variable modulation depth. The relative displacement δp was determined using Eq. (1). In the same figure the black circles give the contrast of the broad fringes from six interferograms with a constant modulation depth. In the latter case the relative displacement δp is equal to the difference between the fractions of the central orders of the individual glass plates. The value of δp was varied from one interferogram to the other using the change in the position of the common axis of the entrance and exit apertures relative to the axis of the interferometer with a common aperture of 50 mm. The continuous curve in Fig. 6 shows the theoretical variation in the contrast over the interferogram with a variable modulation depth. The results shown in Fig. 6 lead to the following conclusions.

When the principal section of the wedge is perpendicular to the plane of rotation, the values of the contrast (the dark circles) are higher than in the case when the principal section of the wedge is parallel to the plane of rotation (the crosses and light circles). In the first case the plane of reflection of the inclined beams does not coincide with the principal section of the wedge where the angle of divergence of the interfering plane waves has the least value. In the second case the plane of reflection and the principal section of the wedge coincide, and the angle of divergence has its highest value of 2α . A reduction in the angle of divergence leads to an increase in the contrast, approaching the contrast of the fringes of the plane-parallel layer.

The experimental and theoretical values of the contrast agree, which confirms the accuracy of the equation of the resonance contour which is considered in the following section.

The resonance contour. The resonance contour of the three-layer interferometer (see Fig. 6) can be derived from the product of the resonance contours of the component layers of the interferometer. This contour describes, with a large degree of accuracy, the variation in the modulation depth when the relative shift of the resonance maxima of the component layers is varied. We will use as the resonance contour of each component layer the Airy function

$$A(k, \gamma) = \left[1 + \frac{\sin^2 \Phi/2}{\text{sh}^2 \gamma/2} \right]^{-1}. \quad (2)$$

The function (2) is normalized so that its resonance maximum is equal to unity. We have used the following notation in (2). The phase difference $\Phi = 2(k - k_0)l$, where k is the wave number and l is the optical thickness of the layer. If δ, δ' are the phase jumps for reflection inside the layer, k_0 is given by $2k_0l + \delta + \delta' = 2p$, where the integer p is the order of the interference. The value of γ is found from the equation $\gamma = \ln R$, where R is the effective energy reflection coefficient of this layer. The quantity γ is the attenuation factor of the interfering waves split inside the layer. The attenuation factor plays a considerable role when determining the parameters of the resonance contour.

An elementary analysis of (2) shows that the resonance minimum is $\text{th}^2 \gamma/2$, and the frequency half-width of the resonance contour is γ . This means that the less the value of γ , the narrower the resonance contour and the lower its minimum.

For convenience in recording the resonance contour of the three-layer interferometer we will assign indices to the Airy functions which distinguish them. Thus, the Airy function of a single layer will be denoted by A_j , where j is the number of the specified layer. The Airy function $A_{j(j+m)}$ defines the resonance contour of the interferometer cavity which comprises the layers of number j and the $j+m$ together with the $(m-1)$ layers between them. The phase difference of the function $A_{j(j+m)}$ is equal to the sum of the phase differences of the specified $(m+1)$ layers and its attenuation factor is increased due to transmission through all the middle boundaries of separation. Taking all this notation into account we can write the resonance contour of the three-layer interferometer in the form

$$T = A_1 A_2 A_3 A_{12} A_{23} A_{13}. \quad (3)$$

It should be noted that Eq. (3) arises from the experimental observations with a three-layer interferometer with adjacent layers of low selectivity (Figs. 1b and c). In this case, when the middle layer has high selectivity (Fig. 1a), Eq. (3) takes the simple form

$$T = A_1 A_2 A_3, \quad (4)$$

since the functions of the complex layers in (3) approach unity in view of the high loss on passing through boundaries of separation with low transmittances. The function (4) is the initial equation for calculating the dependence of the modulation depth of the interferogram on the relative displacement of the fringes of the outer layers. In the case of observation on the maxima of the middle layer, Eq. (4) leads to the contrast equation

$$C = \frac{\left(\operatorname{sh}^2 \frac{\gamma_1}{2} + \cos^2 \pi \frac{\delta p}{2} \right) \left(\operatorname{sh}^2 \frac{\gamma_3}{2} + \cos^2 \pi \frac{\delta p}{2} \right)}{\left(\operatorname{sh}^2 \frac{\gamma_1}{2} + \sin^2 \pi \frac{\delta p}{2} \right) \left(\operatorname{sh}^2 \frac{\gamma_3}{2} + \sin^2 \pi \frac{\delta p}{2} \right)}. \quad (5)$$

Equation (5) holds for plane-parallel layers. We will show below how to calculate the contrast in the case of wedge-shaped plates. According to (5) the contrast of the broad modulation fringes decreases as the relative displacement of the resonance maxima of the outer layers increases. The maximum value of the contrast

$$C_{\max} = \operatorname{cth}^2 \frac{\gamma_1}{2} \operatorname{cth}^2 \frac{\gamma_3}{2} \quad (6)$$

is obtained when the resonance contours coincide, i.e., when substituting $\delta p = 0$. The minimum value of the contrast $C_{\min} = 1$ is obtained on substituting $\delta p = 0.5$, i.e., when the maximum of one contour coincides with the minimum of the other.

In the case of wedge-shaped layers the Airy function (2) is replaced by the following function [3]:

$$A' = \operatorname{th} \frac{\gamma}{2} \left\{ 1 + \frac{1}{2\pi f} \left[\operatorname{arctg} \frac{\sin(2\pi f + \Phi)}{e^\gamma - \cos(2\pi f + \Phi)} + \operatorname{arctg} \frac{\sin(2\pi f - \Phi)}{e^\gamma - \cos(2\pi f - \Phi)} \right] \right\}. \quad (7)$$

In this equation the ratio of the angle of divergence of the plane interfering waves to the angle of the first diffraction minimum is given by the equation $f = 2a/(\lambda/D)$, where D is the width of the rectangular exit aperture. The resonance contour (7) was used to calculate the continuous curve in Fig. 6. It is seen from this figure that the theoretical calculations agree, within the limits of experimental error, with the measured values. The error in the experimental values is due mainly to local deformations of the plates employed. These deformations were observed in the interferograms of fringes of equal thickness. Consequently, the optical thicknesses of the glass plates did not have a pure linear variation. The departure from a linear dependence is determined by the ratio of the area of the working surface of the plate to the area of the exit aperture. In our experiments the area of the working surface of the front plate was 2.5 cm^2 for an area of the exit aperture of 1 cm^2 . The set of dark points in Fig. 6 indicates the fact that the value of the contrast increases as the angle of the wedge decreases so that in the final analysis the contrast is given by Eq. (5).

An interferometer with three thick layers of air and glass and thin-layered alternating coatings of ZnS and cryolite is a multilayer interferometer consisting of purely dielectric layers. The resonance contour of a multilayer interferometer which consists of thin layers is usually determined from the interferogram of equal chromatic orders when working with a continuous spectrum.

A multilayer interferometer with thick layers enables one to investigate the resonance contour in monochromatic light. The advantage of introducing thick layers into the multilayer interferometer is that the angular dispersion regions of thick layers is much less than the dispersion regions of thin layers. In view of this fact the transmission bands of the interferometer are scanned in angular orders, which enables the interference interaction of the interferometer layers to be investigated.

In this investigation this interaction is observed in the form of a change in the modulation depth of the interferogram depending on the relative displacement of the transmission bands of the component layers. It should be noted that this dependence is difficult to obtain for a multilayer interferometer of thin layers since the thin coatings pos-

sess fixed transmission bands. A quantitative analysis of this dependence is of considerable interest when deriving an empirical equation for the resonance contour of a multilayer interferometer.

In conclusion the author thanks Professor F. A. Korolev for his interest and for useful discussions.

REFERENCES

1. M. Khashan, Opt. Commun., vol. 11, p. 213, 1974.
2. M. Khashan, Izv. VUZ. Fizika, no. 4, p. 35, 1970
3. M. Khashan, Izv. VUZ. Fizika, no. 3, p. 73, 1967

1 July 1977

Department of Optics and Spectroscopy